Electronic Supplementary Material (ESI) for Physical Chemistry Chemical Physics.

Quality-dependent performance of hydrophobic ZIF-67 upon high-pressure water intrusion-extrusion process

Eder Amayuelas,[1,*] Luis Bartolomé,[1] Yan Zhang,[1] Juan Miguel López del Amo,[1] Oleksandr Bondarchuk,[2] Artem Nikulin,[1] Francisco Bonilla,[1] Elena Palomo del Barrio,[1, 3] Paweł Zajdel,[4,*] Yaroslav Grosu [1,5,*]

[1] Centre for Cooperative Research on Alternative Energies (CIC energiGUNE), Basque Research and Technology Alliance (BRTA), Alava Technology Park, Albert Einstein 48, 01510 Vitoria-Gasteiz, Spain

[2] International Iberian Nanotechnology Laboratory, Braga 4715-330, Portugal

[3] IKERBASQUE Basque Foundation for Science, Plaza Euskadi 5, 48009 Bilbao, Spain

[4] Institute of Physics, University of Silesia, 75 Pulku Piechoty 1, 41-500, Chorzow, Poland

[5] Institute of Chemistry, University of Silesia, Szkolna 9, 40-006 Katowice, Poland

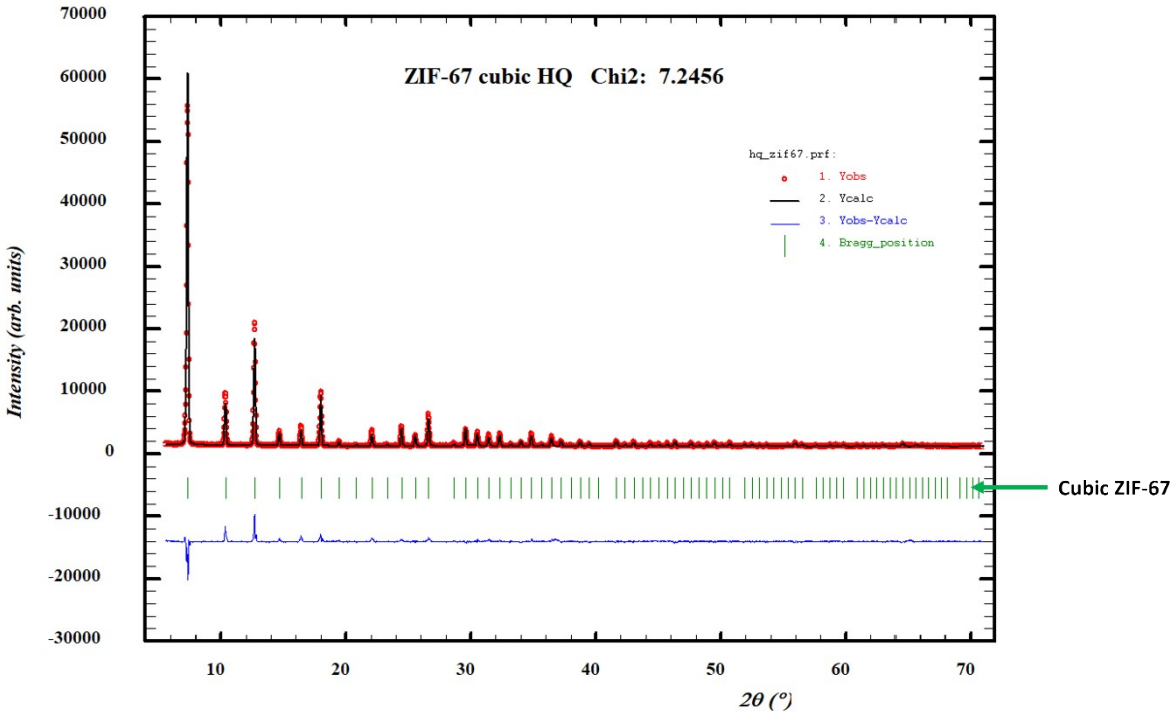

Figure S1. Rietveld refinement of pristine ZIF-67 HQ.

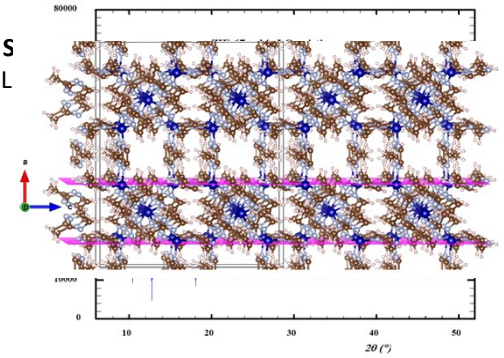

Figure S . Very broad peak at a d-spacing ZIF-67 L 6.3 and 6.7 Å. The possible a disordered ZIF-L-Co phase .)

Figure S4. The ZIF-L-Co phase has a layered character. The size of the layer (depicted using two pink planes is around 6.4 Å).

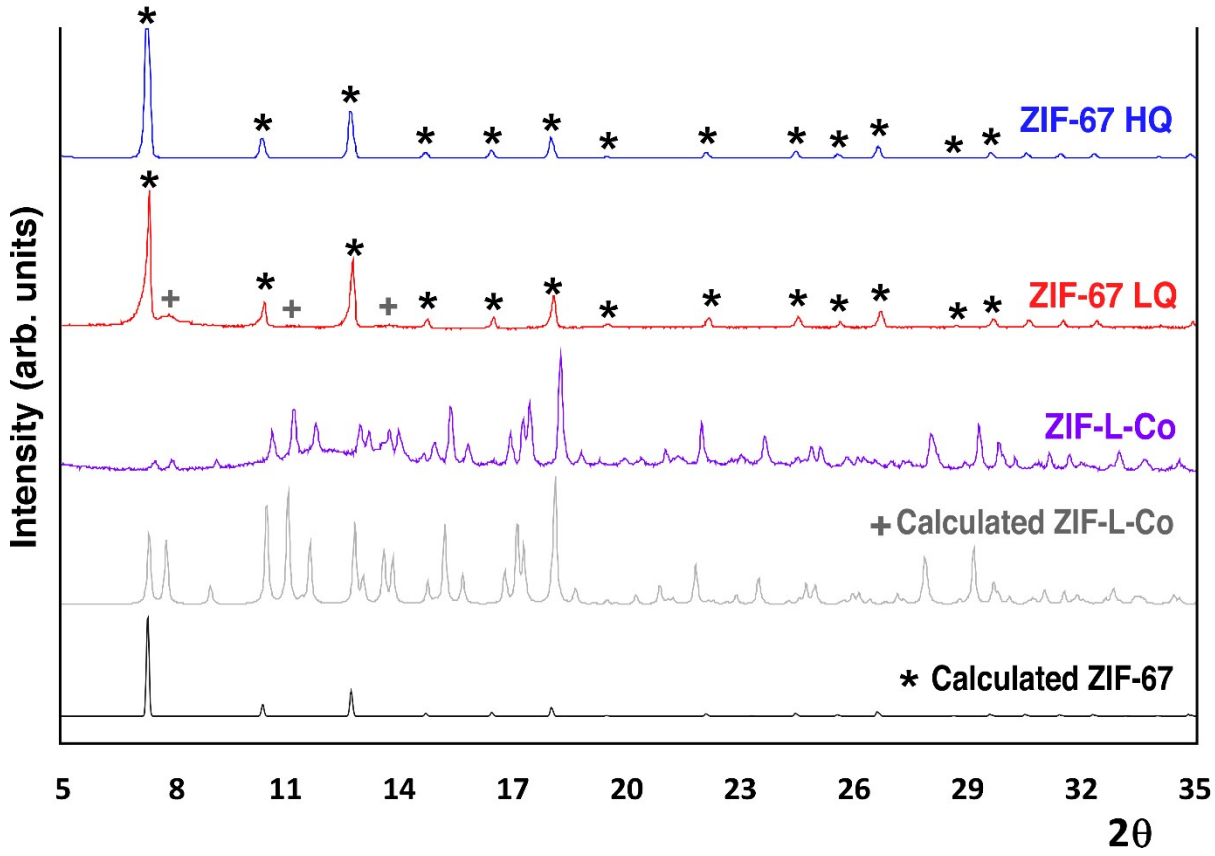

Figure S5. XRD of different ZIF-67 qualities, ZIF-L-Co synthesized sample, theoretical model of ZIF-67 and orthorhombic ZIF-L-Co.

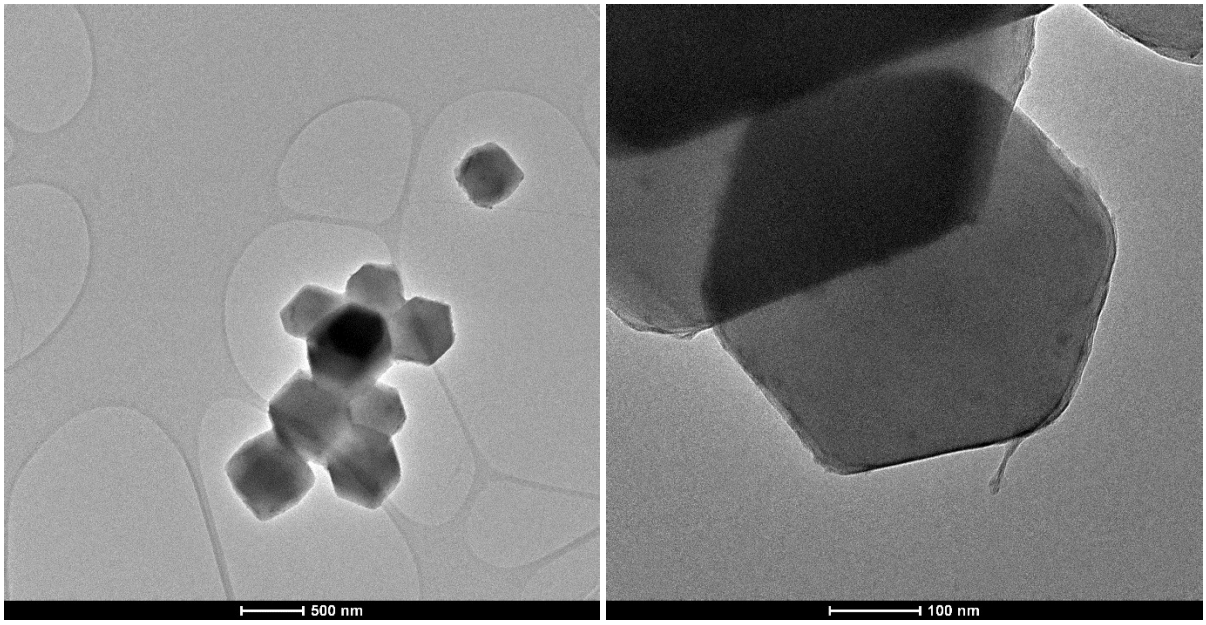

Figure S6. TEM image of the dodecahedral microcrystals of ZIF-67 HQ sample.

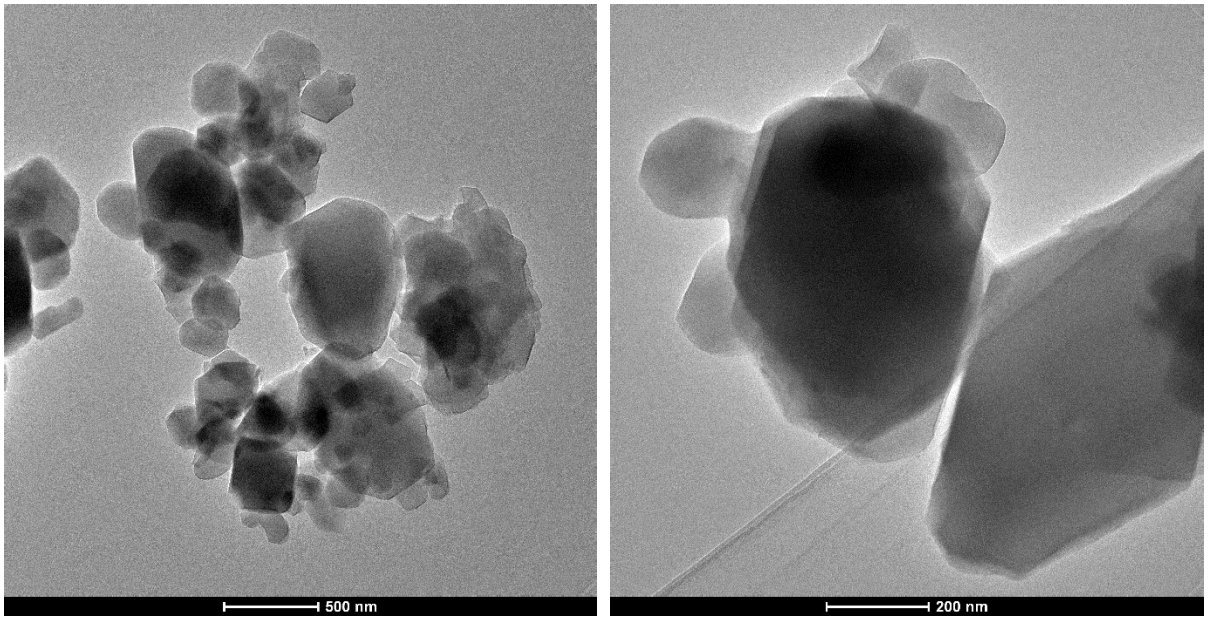

Figure S7. TEM image of the microcrystals of ZIF-67 LQ sample.

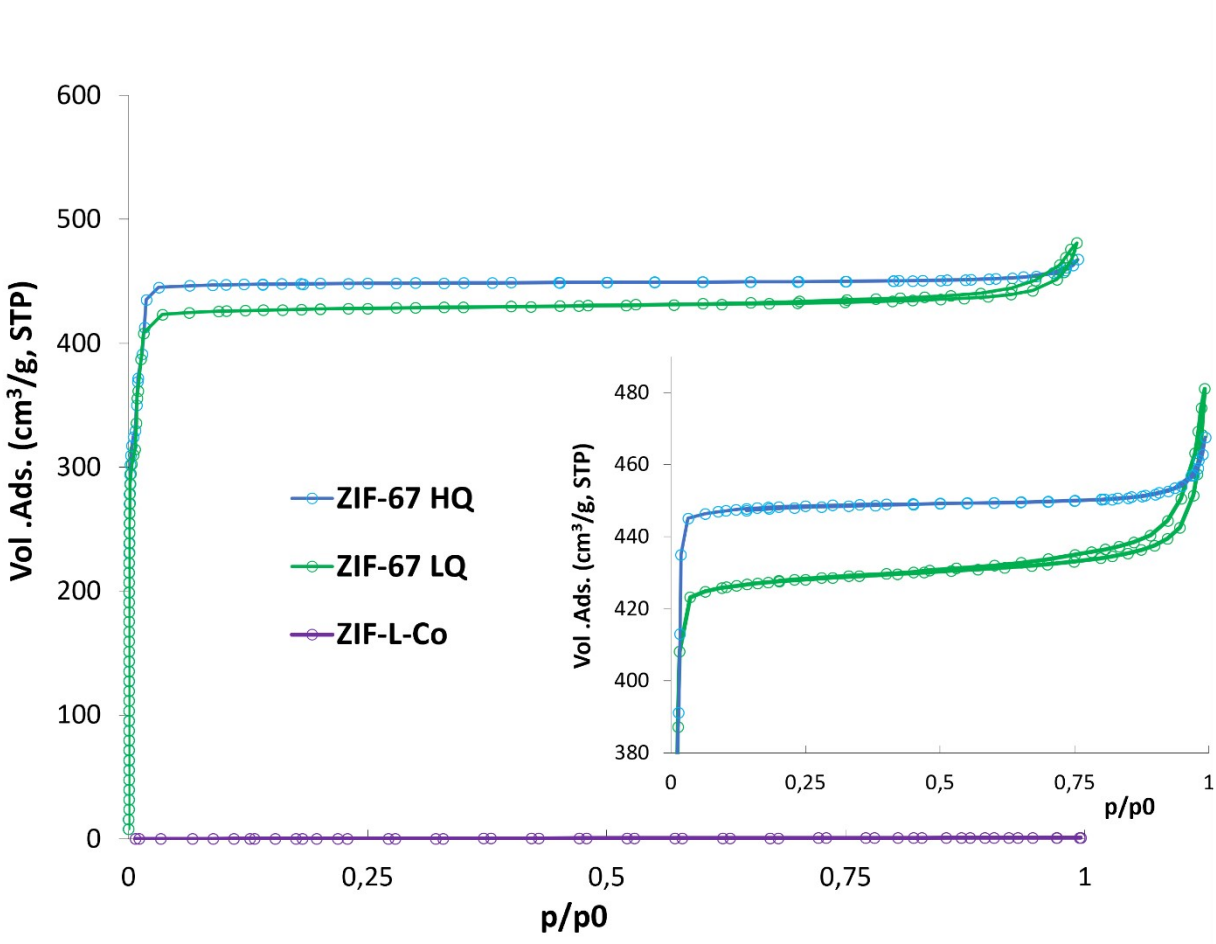

Figure S8. N_2 Isotherms at 77 K of ZIF-67 HQ, LQ and ZIF-L-Co materials. Inset highlights differences between ZIF-67 HQ and LQ isotherms at higher relative pressures.

Material	S_{BET}	Micropore Surface area (t-Plot)	Pore Volume	Micropore volume
ZIF-67 HQ	1745 m^2/g	1732 m^2/g	0.723 cm^3/g	0.687 cm^3/g
ZIF-67 LQ	1648 m^2/g	1616 m^2/g	0.743 cm^3/g	0.647 cm^3/g
ZIF-L-Co	2 m^2/g	m^2/g	0.002 cm^3/g	-

Table S1. Textural values for ZIF-67 HQ and LQ.

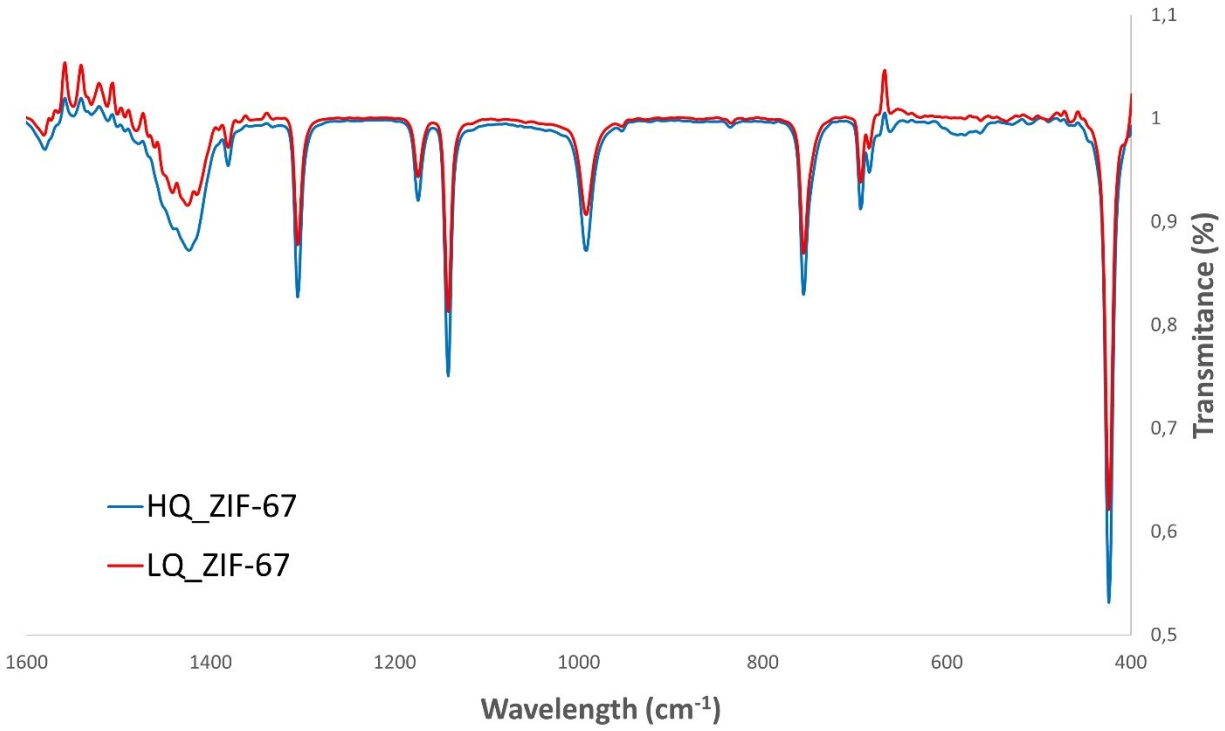

Figure S9. FTIR spectra of pristine ZIF-67 H and ZIF-67 LQ.

Wavenumber [cm^{-1}]	Assignment	Reference
425	Co-N bond	1
693	Out of plane vibration of imidazole ring	3
756	Out of plane vibration of imidazole ring	3
989	C-N bond	2

1141	C-N stretching mode	4
1175	Ring vibration	5
1304	N-H bending mode of imidazole	4
1423	C=C group of imidazole	1
1580	Stretching vibration of imidazole	3

Table S2. Signal Assignments of ZIF-67 HQ and ZIF-67 LQ FTIR Spectra.

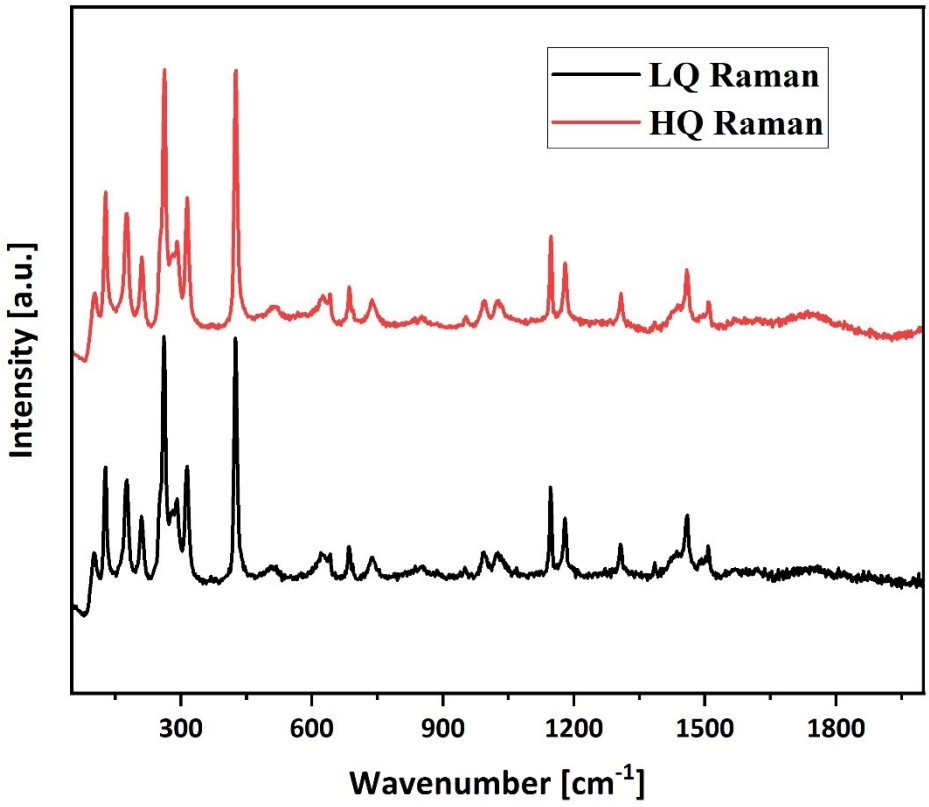

Figure S10. Raman spectra of pristine ZIF-67 HQ and ZIF-67 LQ.

Wavenumber [cm^{-1}]	Assignment	Reference
128	Stretching of Co-N bond	8
175	Co-N bond	10
425	Co-ligand vibration	11
507	Co tetrahedral sites	9

685	C-H in imidazole ring	5,10
735	A1g vibration mode of octahedral sites	9
948	C-H bending	10
992	C-N bond in imidazole	5
1023	C-H bending mode	10
1145	Vibration of C-N	10
1178	Vibration of C-N and N-H	10
1305	Ring expansion of imidazole	10
1384	CH_3 group	10
1456	C-H wagging	10
1508	Vibration of C_4-C_5	10

Table S3. Signal assignments of pristine ZIF-67 HQ and ZIF-67 LQ Raman spectra

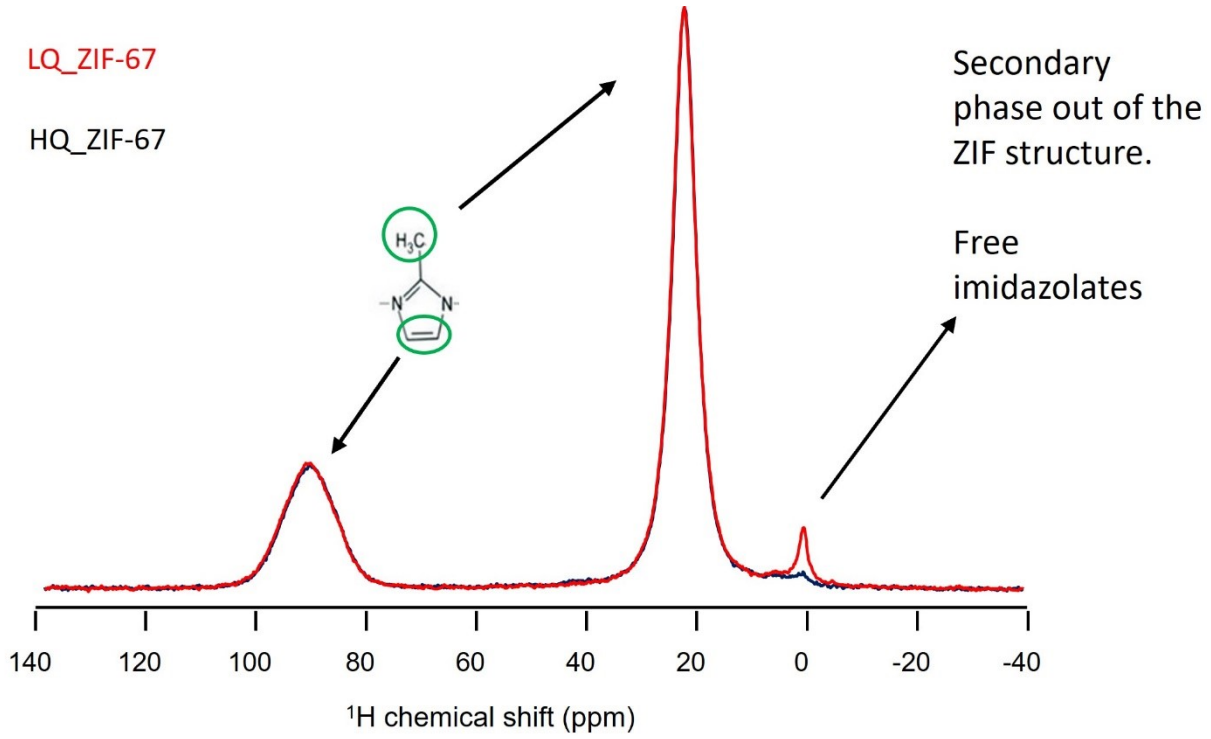

Figure S11. 1H solid state NMR spectra of pristine ZIF-67 HQ and ZIF-67 LQ.

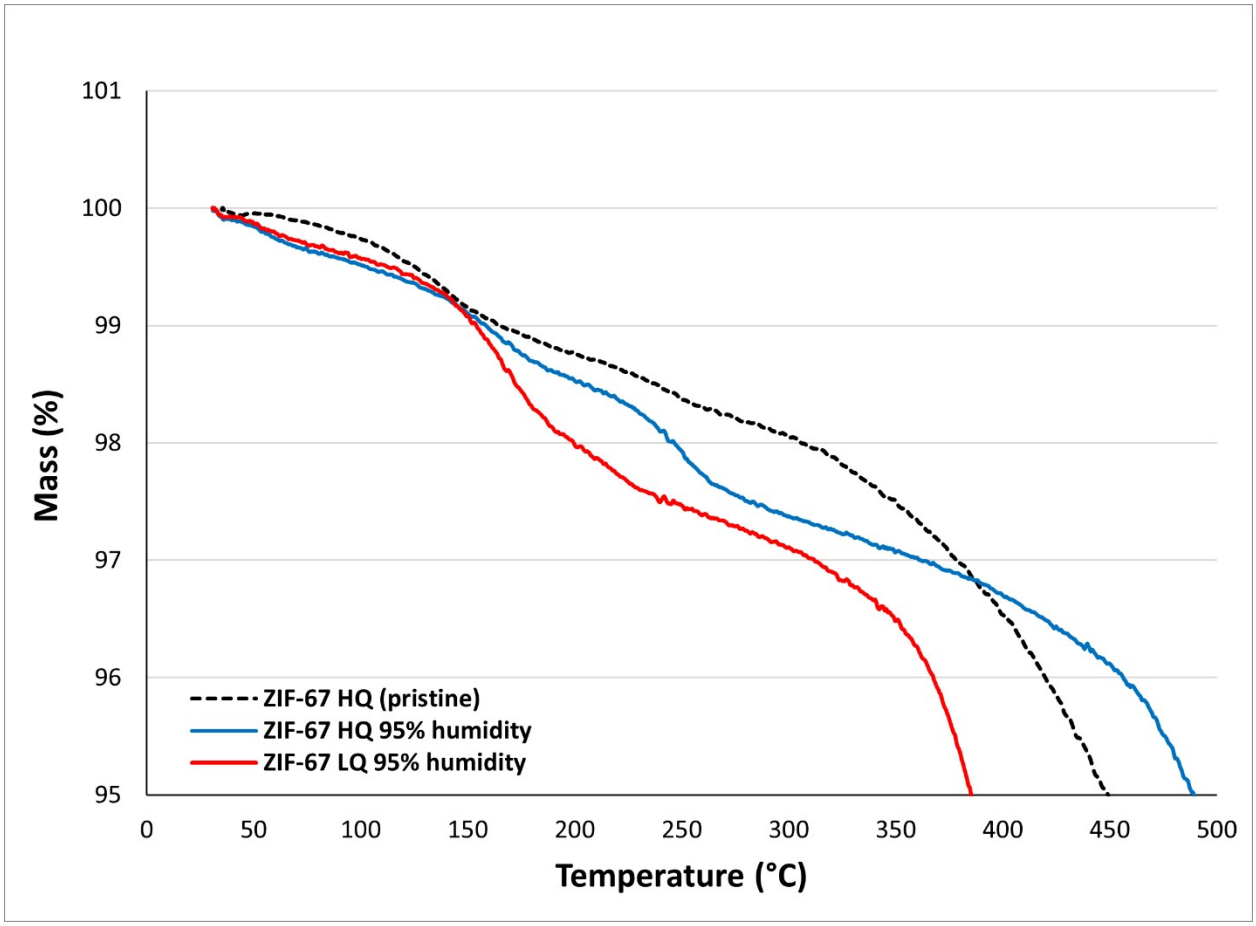

Figure S12. Thermogravimetric decomposition of ZIF-67 HQ and ZIF-67 HQ and LQ after exposition at 95% of humidity.

	Intrusion/extrusion volume - V_{int}/V_{ext} (cm^3/g)									
Material/cycle	**1st**	**2nd**	**3rd**	**4th**	**5th**	**6th**	**7th**	**8th**	**9th**	**10th**
ZIF-67 HQ	0.36/0.36	0.36/0.36	0.36/0.36	0.36/0.36	0.35/0.35	0.34/0.34	0.34/0.34	0.34/0.34	0.33/0.33	0.33/0.33
ZIF-67 LQ	0.31/0.25	0.28/0.25	0,23 /0.23	0.23/0.23	0.21/0.20	0.20/0.20	0.20/0.20	0.22/0.20	0.22/0.20	0.2/0.2

Table S4. Intrusion/extrusion volume values for ZIF-67 HQ and ZIF-67 LQ in all intrusion-extrusion cycles.

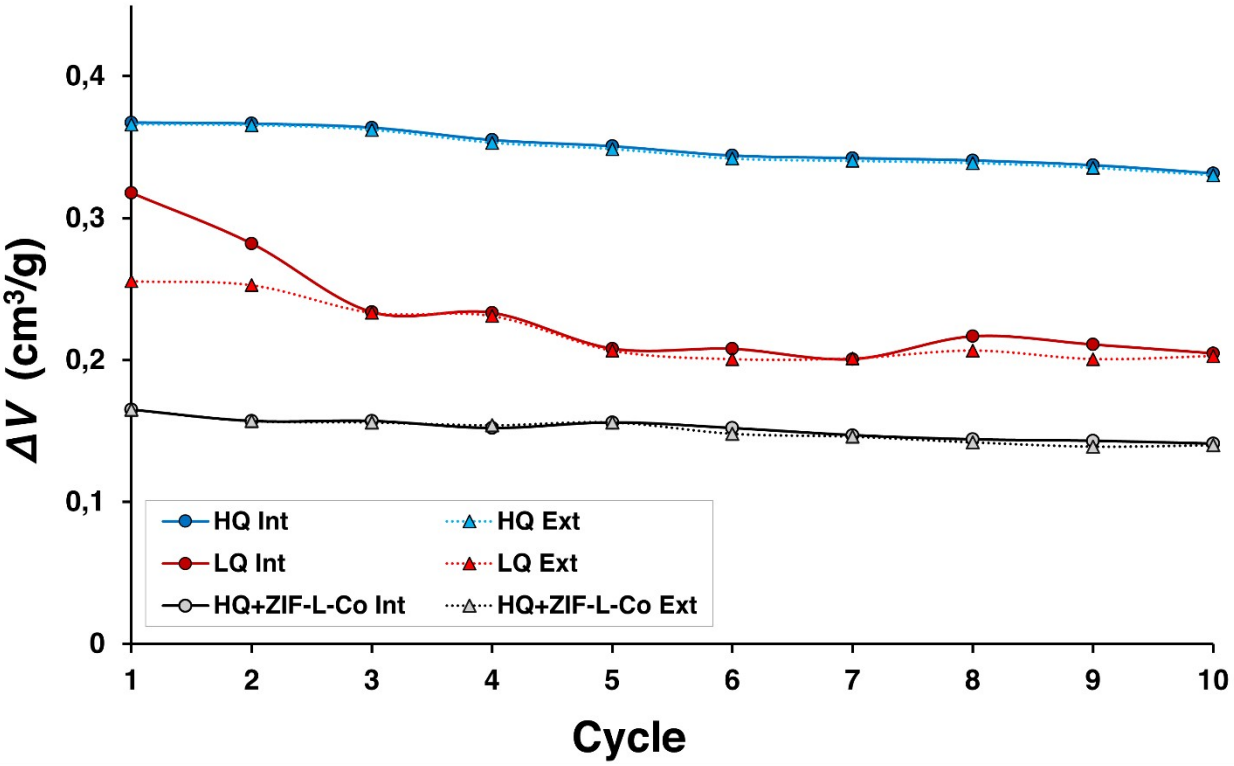

Figure S13. Evolution of V_{int} and V_{ext} during successive cycles of ZIF-67 HQ, ZIF-67 LQ and physical mixture of ZIF-67 HQ+ZIF-L-Co (50% in weight). Note that intrusion volume of the mixture is low since 50 wt% of this sample is a non-porous ZIF-L-Co phase.

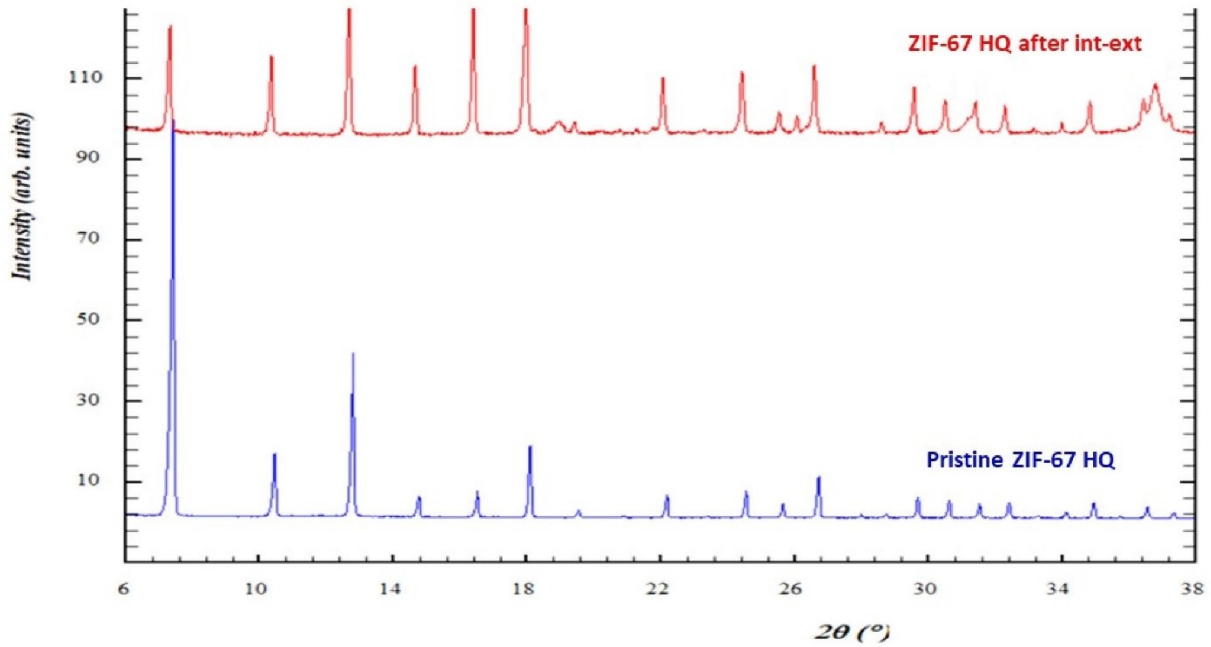

Figure S14. Comparison of XRD patterns of pristine ZIF-67 HQ and ZIF-67 HQ after H_2O int-ext cycles.

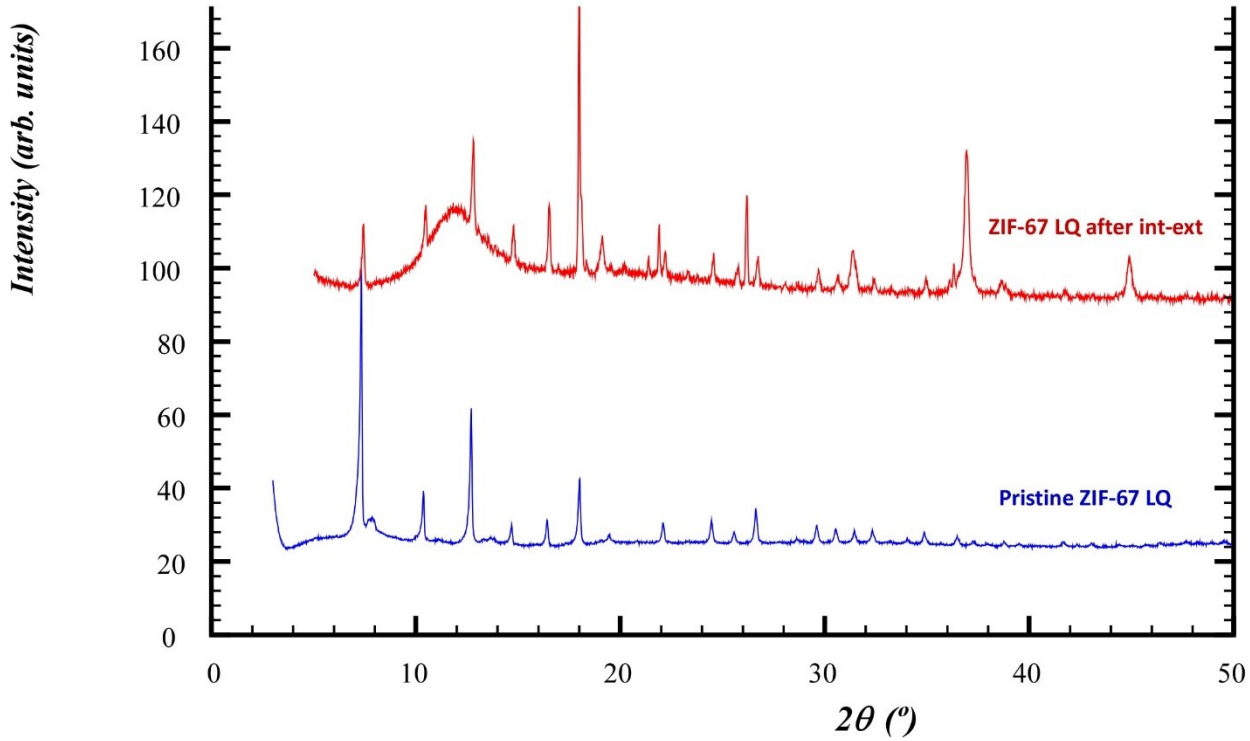

Figure S15. Comparison of XRD patterns of pristine ZIF-67 LQ and ZIF-67 LQ after H_2O int-ext cycles.

Rietveld refinement of tested ZIF-67 samples:

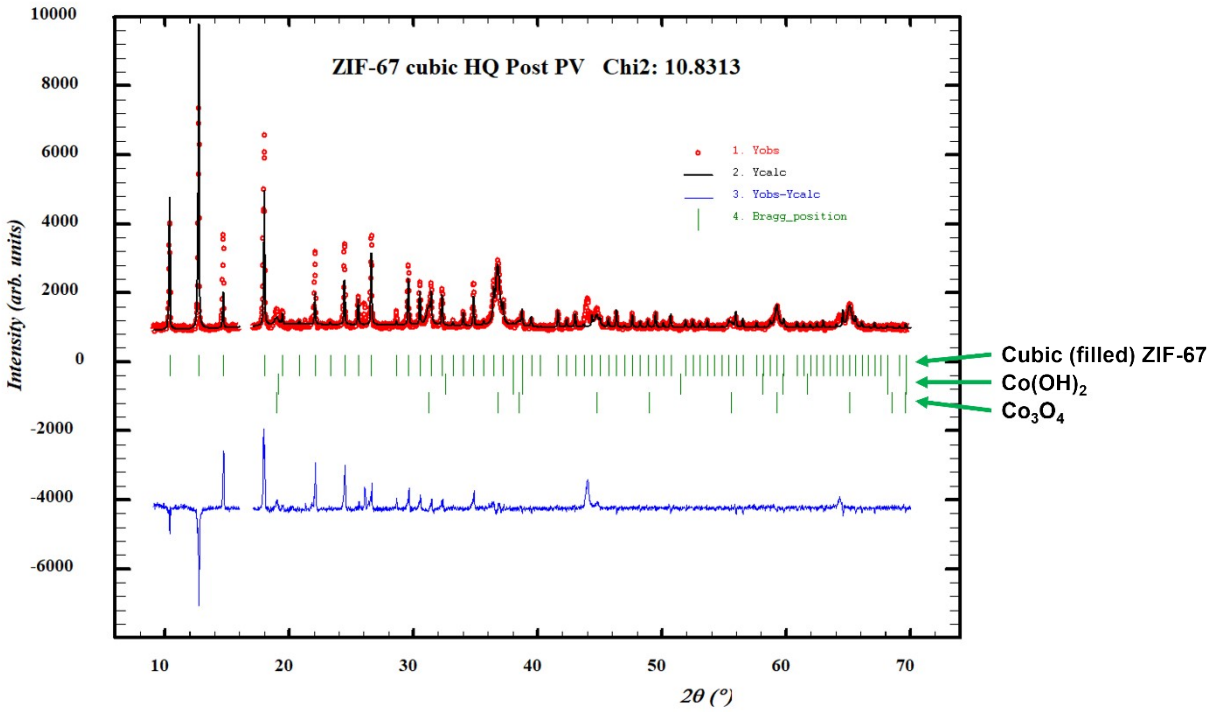

Figure S16. Rietveld refinement of tested ZIF-67 HQ.

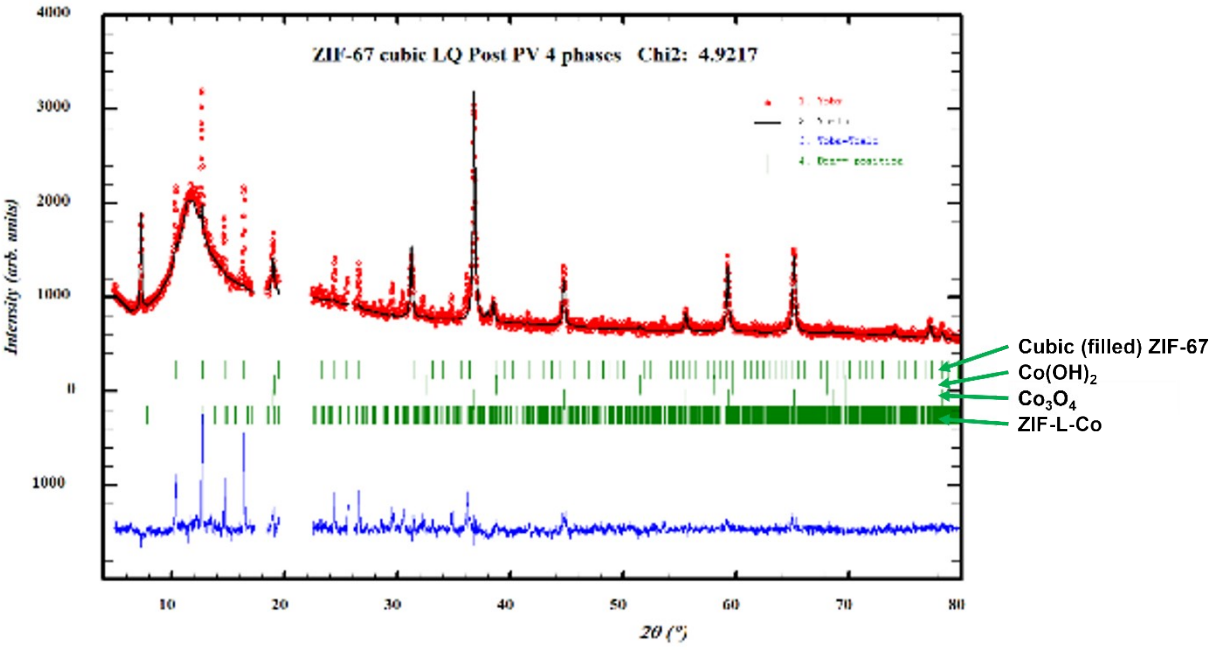

Figure S17. Initial Rietveld refinement of the ZIF-67 LQ tested sample. There are several peaks of the ZIF-67 phase which are severely scaled down relatively to the first (110).

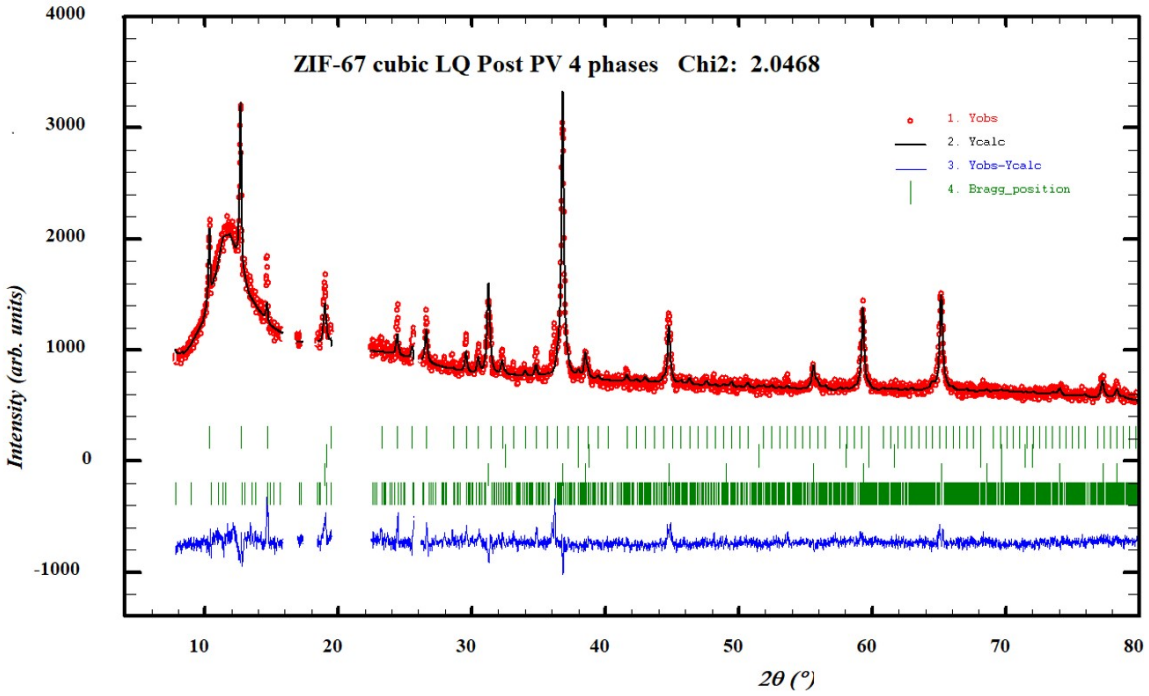

Figure S18. Rietveld refinement used for the qualitative refinement. The (110) and (310) of the SOD phase have been excluded.

Analysis of the LQ sample after cycling has been carried out in several steps. Firstly, a quick overview of the diffractogram revealed the presence of a second strong phase which was identified as a cubic Co_3O_4. There were no clear reflections from $Co(OH)_2$ or ZIF-L type MOF but there were left in the refinement for testing. Unfortunately, the 4 phases did not describe all the additional reflections which were located at the positions (in Å) (2Θ values in degrees) of: 4.95 (17.89), 4.16 (21.30), 4.07 (21.81), 3.41 (26.10), 2.48 (36.02), 2.49 (36.22). Indexing the extra phases was not successful, which probably indicates the system has multiple phases.

The two main cubic phases of the cycled LQ sample: SOD and Co_3O_4 were treated the following way. First, the regions with the unassigned peaks were excluded from the refinement. Then, a pattern matching was performed to get lattice parameters of ZIF-67 and Co_3O_4.

Next, the profile parameters were fixed and the Rietveld analysis was attempted, which resulted in a very bad fit (Figure S12). The reason behind the suppression of intensities of several reflections from the ZIF-67 was a very low intensity of the (110) reflection, which lowered other calculated intensities.

The lowering of the intensity of (110) in other MOF with sodalite topology is related to the filling of the internal pore. Therefore, in the figures, the phase is referred as ZIF-67 (filled). On this basis, we concluded that the decomposition of ZIF-67 into Co_3O_4 must leave byproducts inside the cage. Additionally, a quick inspection of HQ tested material also revealed a similar decrease in the intensity of the (110) reflection.

We were not able to model the filling of the cage, and for the purpose of qualitative refinement, the (110) and (310) of ZIF-67 were also excluded from the fit. The exclusion partially sorts out the misfit as the other reflections do not change intensities to a large extent under the filling of the central cage. The final fit is presented in Figure S13. The phase contents in weight fractions were 38(1) % of the SOD phase and 60(1)% of Co_3O_4. The remaining 1.5(3) percent was a small possible contribution from Co(OH)2.

The inspection of the diffractogram for the tested HQ sample revealed a strong decrease in the intensity of the (110) peak. The Fourier difference did not show any peaks related to the missing scattering density and in fact the negative and positive differences were at the same level. Therefore, similarly to the LQ case, peaks with strong variations of intensity (110) and (310) were also excluded from the fit.

The HQ systems were described by 3 phases: SOD, $Co(OH)_2$ and Co_3O_4. In the case of HQ material, two additional unidentified peaks were found at d-spacing (in Å) (2Θ values in degrees) of: 3.41 (26.06), 2.05 (44.00). They partially overlap with peaks from the LQ tested material, which possibly indicates the same extra phase.

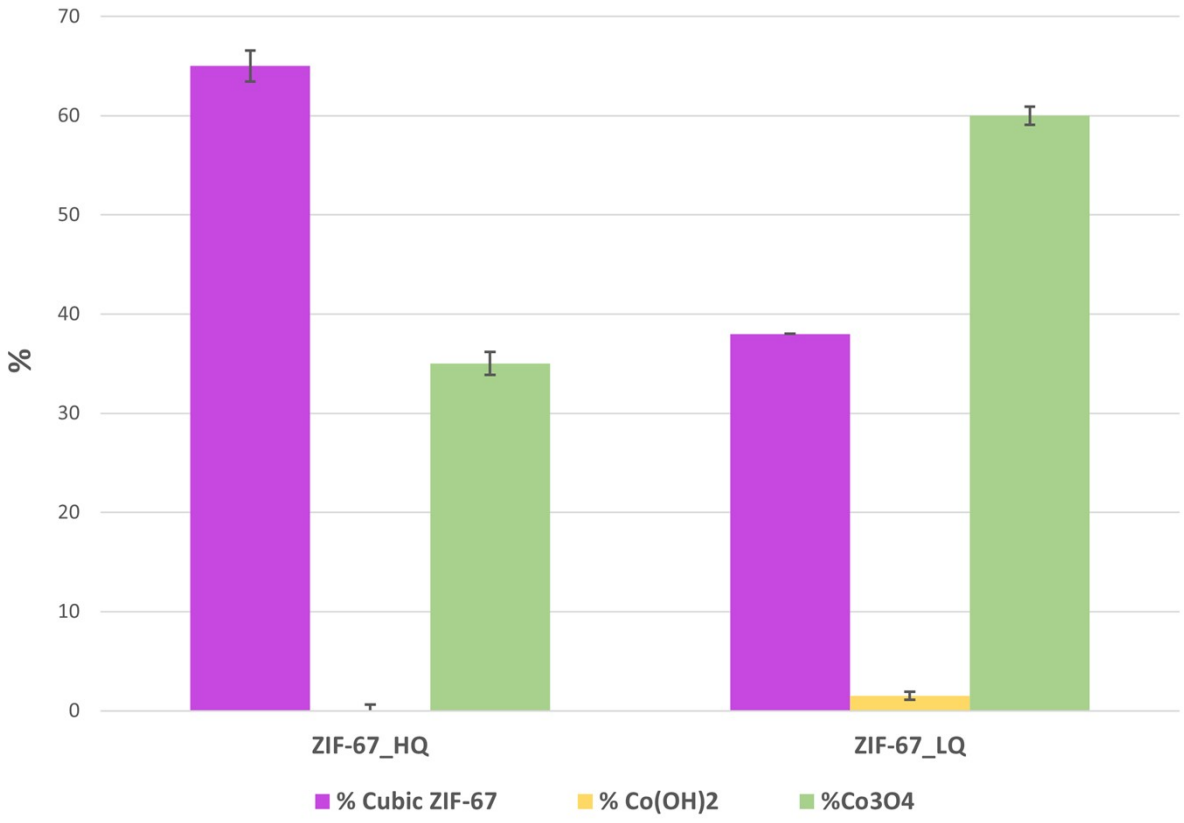

Figure S19. Histogram of degradation products proportion for each ZIF-67 tested sample.

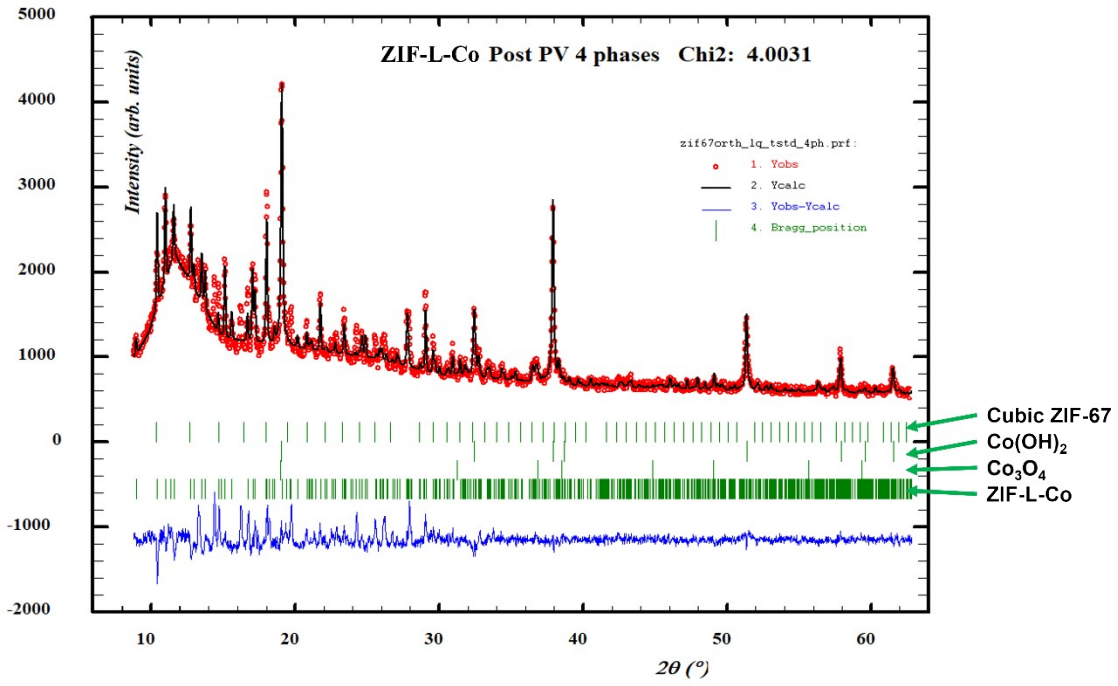

Figure S20. Overview of the current stage of the refinement of the second sample. The dominating phase is $Co(OH)_2$. Next, we have ZIF-L-Co. Almost no contribution from Co_3O_4 or cubic ZIF-67.

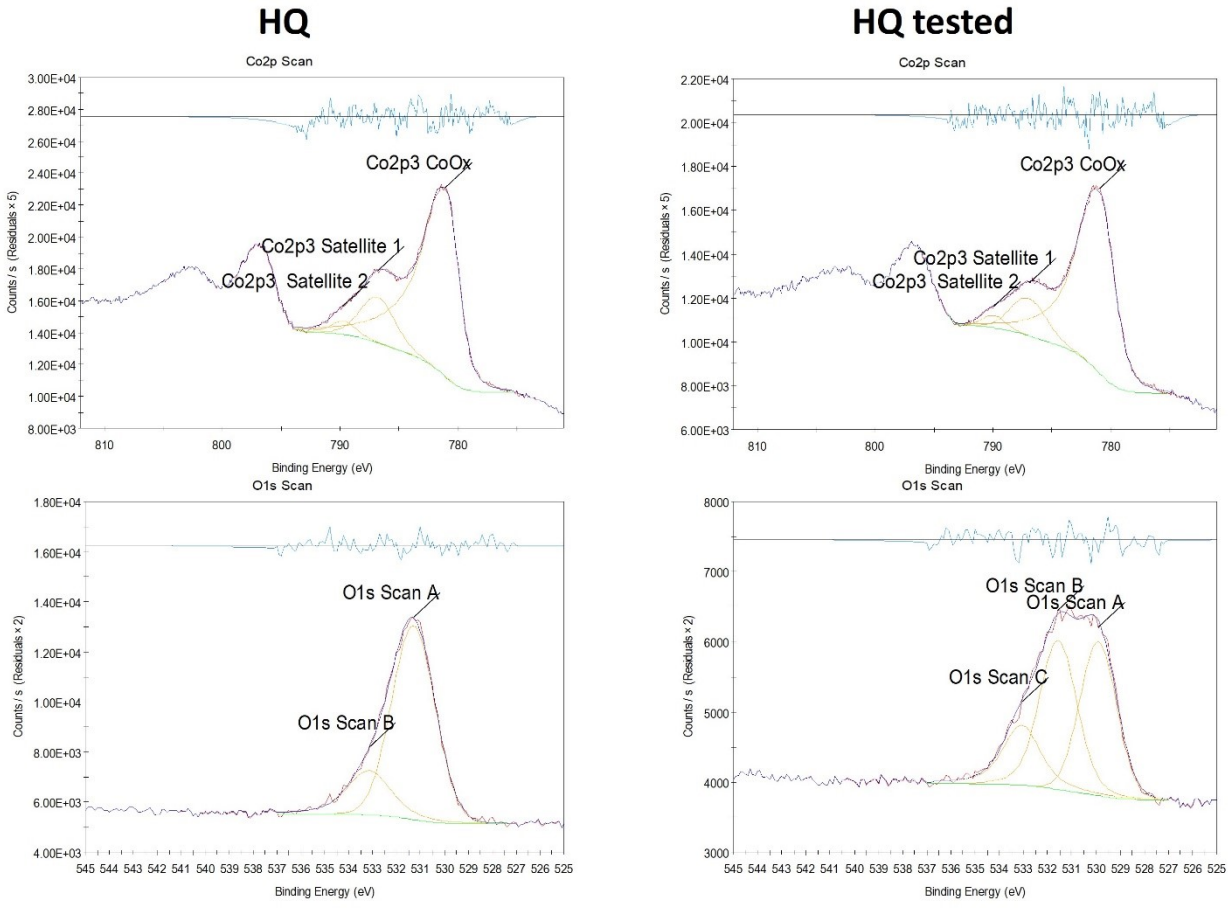

Figure S21. XPS spectra of pristine ZIF-67 HQ and tested one. Co2p spectrum stays virtually the same after testing. The satellite peak at ~786 eV is characteristic of Co^{2+} in CoO and $Co(OH)_2$ compounds.[10] In the O1s spectrum after

testing appears additional peak at ~530 eV, which is the typical position of the peak in metal oxides thus indicating oxidation of Co at least on the surface.

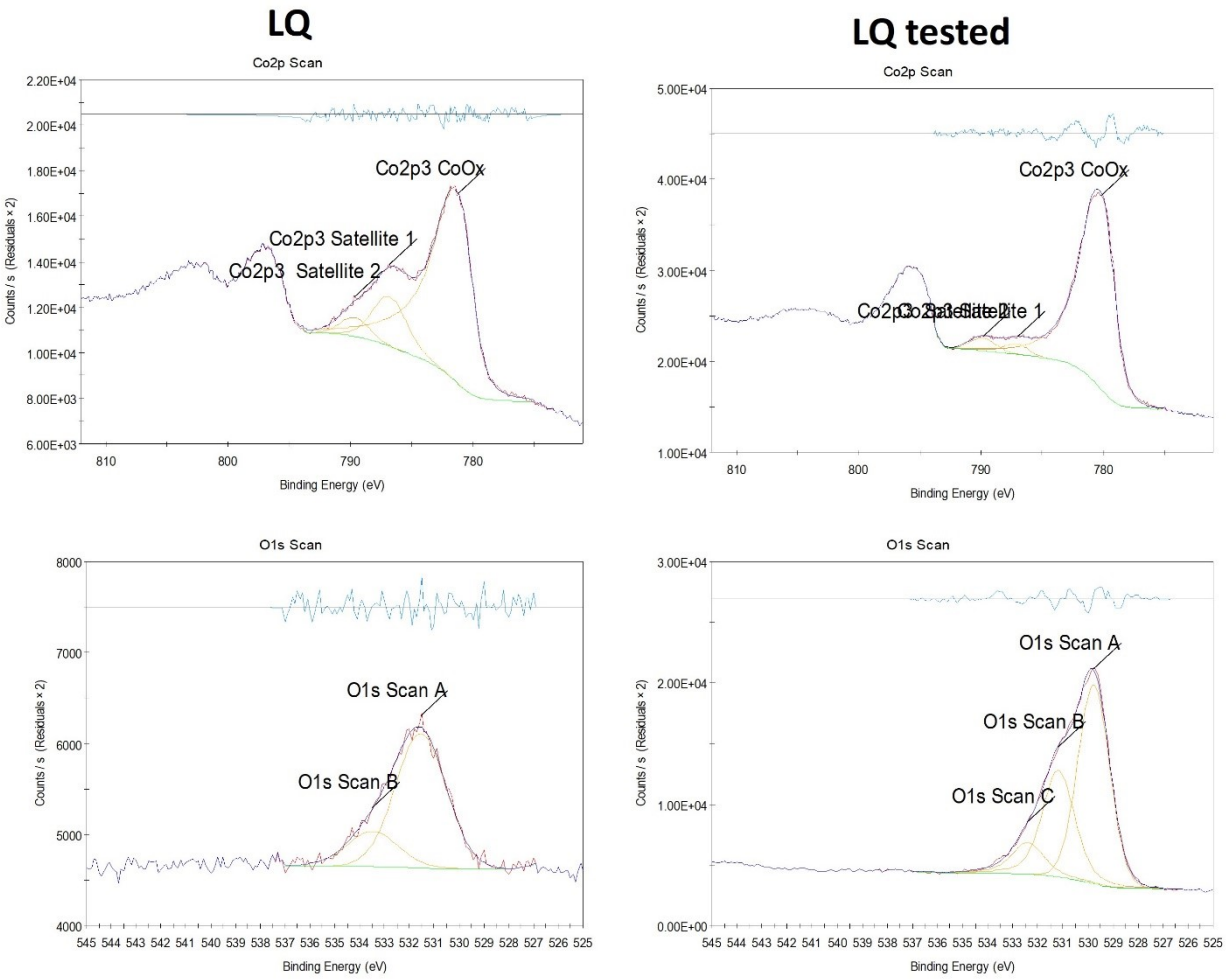

Figure S22. XPS spectra of pristine ZIF-67 LQ and tested one. The satellite peak at ~786 eV is gone after testing, The satellite pattern characteristic of Co_3O_4.[10] In O1s spectrum after testing appears an additional peak at ~530 eV, similar to that in "HQ tested". Besides Co/O ratio drastically increased after LQ sample testing indicating strong oxidation of Co.

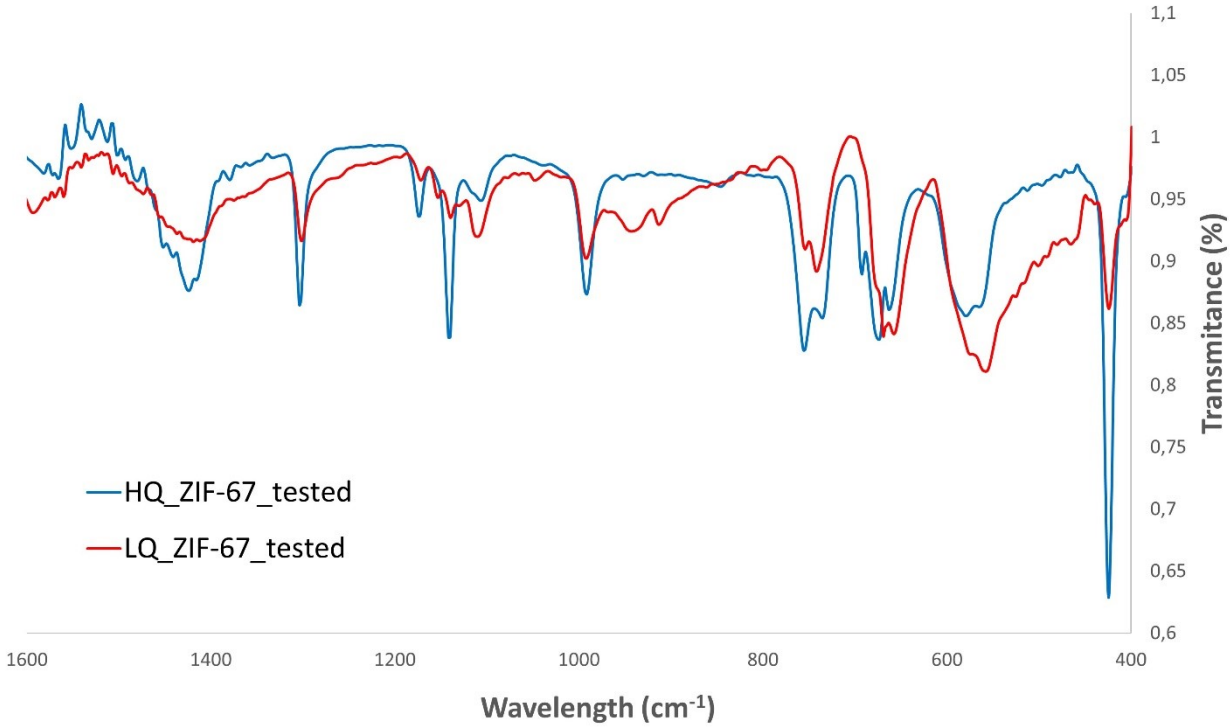

Figure S23. FTIR spectra of tested ZIF-67 HQ and ZIF-67 LQ.

Wavenumber [cm^{-1}]	Assignment	Reference
576	Co-O stretching vibration in Co_3O_4	11
663	Co-O stretching vibration in Co_3O_4	11
558	Co(II)-O stretching	12
677	Co(III)-O stretching	12

Table S5. Signal assignments of tested ZIF-67 HQ and ZIF-67 LQ FTIR spectra

References:

1. M. Afkhami-Ardekani, S. Doaee and S. Rostamnia, "Solvent-Free Mechanochemical Preparation of Metal-Organic Framework ZIF-67 Impregnated by Pt Nanoparticles for Water Purification", Catalysts, **13**(1), 9 (2023)

2. L. Zhang, A. Wu, M. Tian, Y. Xiao, X. Shi, H. Yan, C. Tian and H. Fu, "2-D porous Ni3N–Co3N hybrids derived from ZIF-67/Ni(OH)2 sheets as a magnetically separable catalyst for hydrogenation reactions", Chemical Communications, **79**, (2018).

3. Y. Hu, X. Song, Q. Zheng, J. Wanga and J. Pei, "Zeolitic imidazolate framework-67 for shape stabilization and enhanced thermal stability of paraffin-based phase change materials", RSC Advances, **18**, (2019).

4. L. Ma, X. Zhang, M. Ikram, M. Ullah, H. Wu and K. Shi, "Controllable synthesis of an intercalated ZIF-67/EG structure for the detection of ultratrace Cd^{2+}, Cu^{2+}, Hg^{2+} and Pb^{2+} ions", Chemical Engineering Journal, **395**, 125216 (2020**)**.

5. A. Di Santo, H. Perez, G. Echeverria, O. E. Piro, R. Iglesias, R. E. Carbonio, A. B. Altabef and D. M. Gil, "Exploring weak intermolecular interactions in thiocyanate-bonded Zn(ii) and Cd(ii) complexes with methylimidazole: crystal structures, Hirshfeld surface analysis and luminescence properties", RSC Advances, **8**(42):23891-23902 (2018).

6. M. N. Jackson, M. K. Kamunde-Devonish, B. A. Hammann, L. A. Wills, L. B. Fullmer, S. E. Hayes, P. H.-Y. Cheong, W.- H. Casey, M. Nyman and D. W. Johnson, "An overview of selected current approaches to the characterization of aqueous inorganic clusters", Dalton Trans.,**44**, 16982-17006 (2015).

7. M. Wu, S. Chen, A. Soomro, et al, "Investigation of synergistic effects and high performance of La-Co composite oxides for toluene catalytic oxidation at low temperature", Environ Sci Pollut Res, **26**, 12123–12135, (2019).

8. G. Kumari, K. Jayaramulu, T. K. Maji and C. Narayana, "Temperature Induced Structural Transformations and Gas Adsorption in the Zeolitic Imidazolate Framework ZIF-8: A Raman Study", J. Phys. Chem. A, **117(**43), 11006–11012 (2013).

9. H. Yoon, A. Xu, G. E. Sterbinsky, D. A. Arena, Z. Wang, P. W. Stephens, Y. S. Meng and K. J. Carroll, "*In situ* non-aqueous nucleation and growth of next generation rare-earth-free permanent magnets", Phys. Chem. Chem. Phys**.**,**17**, 1070-1076 (2015).

10. M.C. Biesinger, B.P. Payne, A.P. Grosvenor, L.W.M. Lau, A.R. Gerson, and R.S.C. Smart, "Resolving surface chemical states in XPS analysis of first row transition metals, oxides and hydroxides: Cr, Mn, Fe, Co and Ni," Appl Surf Sci, **257**(7), 2717–2730 (2011).

11. F. Zhang, C. Yuan, X. Lu, L. Zhang, Q. Che, and X. Zhang, "Facile growth of mesoporous Co3O4 nanowire arrays on Ni foam for high performance electrochemical capacitors," J Power Sources, **203**, 250–256 (2012).

12. E.A.A. Aboelazm, G.A.M. Ali, and K. Feng Chong, "Cobalt Oxide Supercapacitor Electrode Recovered from Spent Lithium-Ion Battery" Chemistry of Advanced Materials, **3**(4) 67-74 (2018).